SOUND PENETRATION INTO A SLOPING OCEAN FLOOR

John F. Miller[a], Michael D. Collins[b], Hassan Ali[c], Juan I. Arvelo[d], Anton Nagl[d], and Herbert Uberall[d]

[a]Singer Co., Link Simulation Systems Division, Silver Spring, MD 20910
[b]The Technological Institute, Northwestern University, Evanston, IL 60201
[c]NORDA, NSTL, MS 39529
[d]Physics Department, Catholic University of America, Washington, DC 20064

Abstract. A coupled-mode code developed by us recently[1,2] is used to calculate sound propagation in a bottom-limited, range dependent ocean environment with vertical sound speed gradients. The latter are shown to influence decisively the character of bottom penetration. For the case of up-slope propagation over a continental shelf, previous studies[3,4] that employed codes with isovelocity bottoms showed that upon mode cutoff in the water, sound penetrates into the bottom and disappears in the depth. We demonstrate that for upward-refracting bottom gradients, as often present in sediments, sound will continue propagating shoreward through the ocean bottom beyond the water-cutoff point. A corresponding calculation employing a parabolic-equation (PE) code corroborates these results; it is also used to study the propagation of a Gaussian sound pulse, and the penetration and channeling of sound energy in the bottom where the upward-refracting gradient causes it to reradiate back up into the water, ahead of the water-borne pulse. Bottom channeling can result in the registration by bottom-mounted receivers of signals which have originated in the ocean and traveled up the continental shelf, at locations closer to shore than expected on the basis of water-borne propagation alone.

In the earlier acoustic literature, the topic of upslope sound propagation in an ocean wedge with penetrable bottom has received attention solely in the case of an isovelocity fluid wedge and bottom. Jensen and Kuperman[3] first tackled this problem using the parabolic equation approximation; of the several later investigations, one may mention the mostly analytic studies by Pierce[5,6], and the use of the "slab model" (a succession of constant-depth regions forming a staircase-like bottom) by Evans[4], whose results showed that a coupled-mode approach is applicable, with the wedge-trapped modes cutting off successively while propagating upslope. Each cutting-off mode transfers a considerable amount of energy into the "continuous-spectrum" modes that are not trapped, but propagate into the bottom and which may thus be called "radiating modes". The assumption of an isovelocity bottom makes this bottom penetration appear like a discrete "ray-bundle refraction" of sound energy downward into the bottom (although this

refraction does not correspond to that of a conventional ray picture, but occurs separately for each of the individual modes); the energy then propagates steeply downwards into the bottom[3-6] and gets lost in the depths. In this case, it thus appears that signals originating out in the ocean and traveling shorewards up the continental slope cannot be received any closer to shore than the cutoff point of the last mode in the water wedge.

We have found, however, using a coupled-mode code,[1,2] that when the basement includes a surficial sediment layer with a realistic, upward-refracting sound speed profile, the resulting acoustic field is quite different. The normal-mode model used for our calculation is based on that of Nagl et al.[7] but was considerably extended for the present purpose[1], to wit:

(a) sediment layers with different densities and variable sound velocities have been included in the code, as well as both first and second order mode coupling terms;

(b) the continuous-spectrum modes have also been included, albeit in a discretized form by introducing, following Evans[4], a mathematical pressure release boundary underneath the basement.

Our calculations are carried out for the bathymetry shown in Fig. 1. From the 25-Hz source (at 112m depth) inward, isovelocity water with a sound speed c = 1,500m/sec, a density ratio = 1, and a depth of 200m, reaches over a 5000m range, then slopes linearly upwards to a depth of 60m at a range of 10,173m (i.e., with a slope of 1.55°), remaining flat from there onwards. As our Case 1, we assume an isovelocity basement of c_B = 1704.5 m/sec and ρ_B = 1.15 underlying the water wedge. For our Case 2, we introduce a linear, upward-refracting gradient in the water such that c = 1,500m/sec at the water surface, and 1,700m at a depth of 200m. For Case 3, we assume the same basement, but reaching from a depth of 300m downward; a sediment layer is taken to lie between the water wedge and the basement, and to have a constant sound speed gradient g = 0.85 sec^{-1}, and constant values of ρ_S = 1.15, and of c_S = 1704.0 m/sec at its interface with the basement. In all cases, we take the deep pressure-release boundary to be at 1200m depth, together with a basement attenuation constant of ε = 0.84 x 10^{-3} nepers/m in order to eliminate spurious reflections from this boundary.

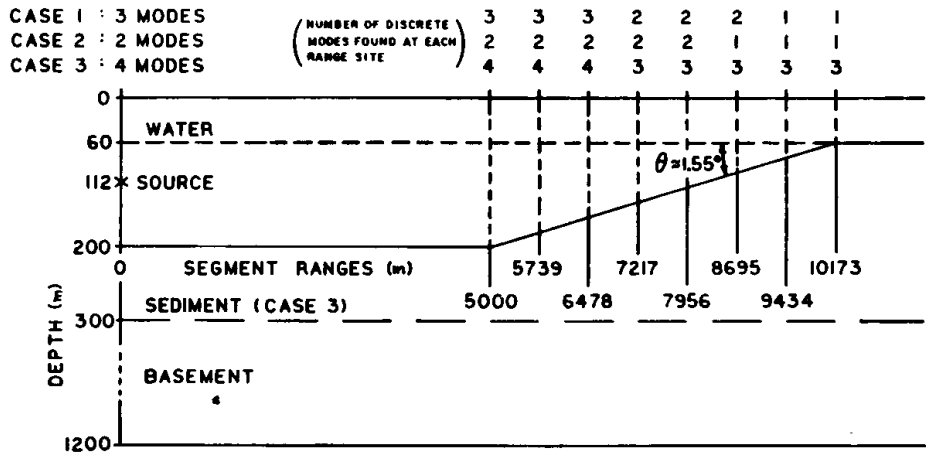

Fig. 1. Geometry of ocean wedge, sediment, and basement assumed in the present study.

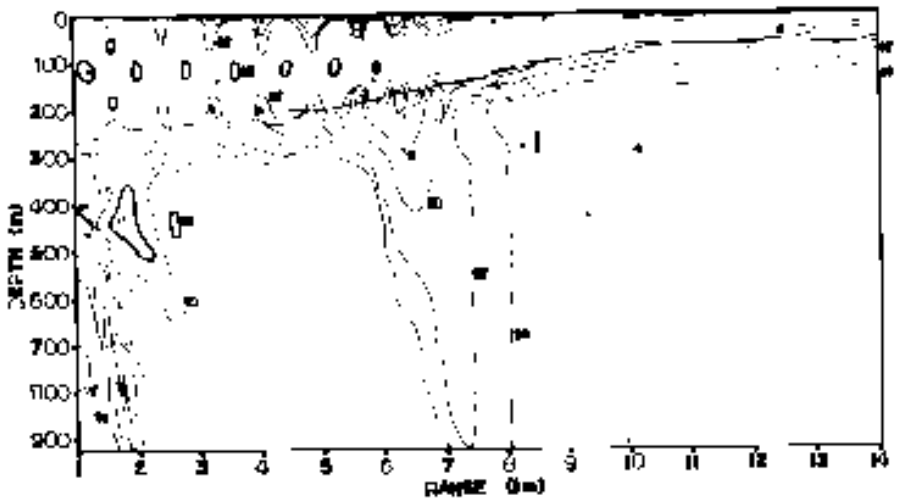

FIG. 2. Contour plot of the propagation loss (in dB) for Case 1 (two isospeed layers), using 22 modes.

Our Case 1 (isovelocity sediment/basement) corresponds exactly to that considered by Evens[4]. Three trapped modes are present in the source interval: one cuts off at a range around 7000m; another cuts off near 9000m but the source depth has been chosen to coincide with a null of this mode so that it does not contribute to our acoustic field. The last mode does not cut off but propagates into the flat region at the top of the wedge.

Our results for this case are shown in Fig. 2. A total of 36 modes exist (three trapped and 33 radiating ones at the source); the sound field of Fig. 2 was calculated using 22 modes, although the results were seen to stabilize with only 15 or so modes. At the cutoff point of the mentioned mode (near 7000m), the sound is coupled into the basement, and owing to the isovelocity profile, is radiated steeply downwards, only to be lost in the depths. The results of Fig. 2 correspond closely to those of Evens.[4] Quite similar results are seen in Fig. 3 which corresponds to Case 2 (gradient in the water, isovelocity bottom).

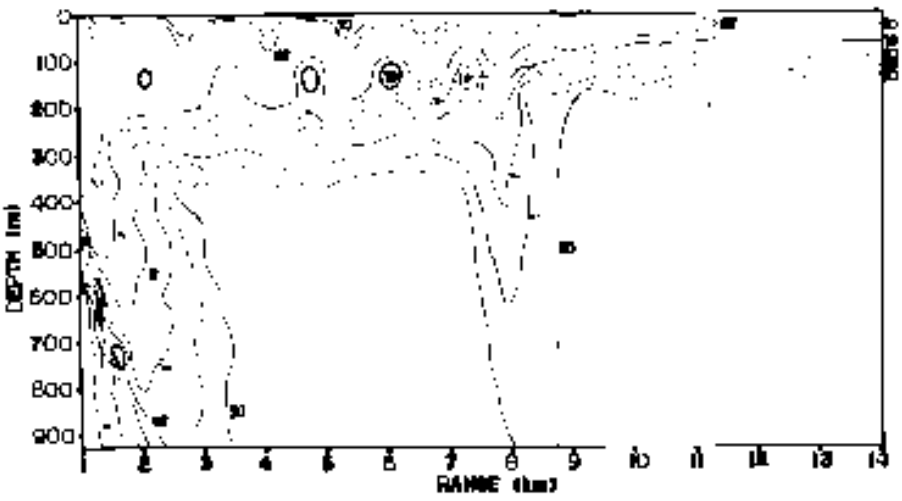

Fig. 3. Contour plot of the propagation loss (in dB) for Case 2 (upward-refracting water column), using 22 modes.

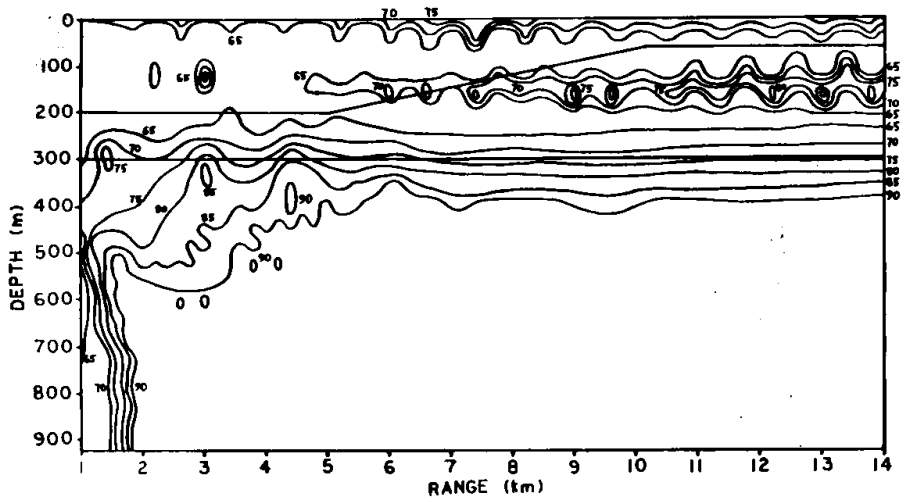

Fig. 4. Contour plot of the propagation loss (in dB) for Case 3 (three layers with upward-refracting sediment).

The situation changes for the bottom-gradient Case 3 of Fig. 1 (upward-refracting sediment layer). Four trapped modes are present here in the source interval; one of these cuts off near a range of 7000m while the three remaining ones continue propagating into the flat region at the top of the wedge. Figure 4 shows the acoustic field for this case, using 22 modes as before[2]. This time, near the cutoff point of the mentioned mode (which, as before, was strongly excited at the assumed source depth), no downward-propagating radiaton "tongue" appears. Instead, the radiation spreads into the sediment in two nearly horizontal layers, the top layer dipping just below the water-sediment interface, the bottom layer delving somewhat deeper, but never reaching as far down as the sediment-basement interface. We conclude that the cutting-off of a mode propagating upslope in the wedge leads to a transfer of its acoustic energy into the bottom, but in such a way that the sediment-borne sound continues traveling upslope rather than downwards into the basement. This indicates that receivable signals can be carried close to shore, past the cutoff points of water-borne modes, provided they are registered by appropriate bottom-mounted receivers.

In order to corroborate this important result, we performed an independent calculation of the sound field corresponding to the environment of Case 3, based on a parabolic-equation (PE) code developed at NORDA[8], which solves numerically the parabolic approximation of the Helmholtz equation by a finite-element technique. The code treats various fluid environments and is capable of handling range dependence, as well as vertical sound speed gradients in the fluids. It consists of two parts:

(a) The code FEPE solves time harmonic problems, using a one-way in range approximation of the Helmholtz equation and solving it over small range-independent increments. The range dependent environment is dealt with by allowing the matrices involved to be updated as the environment changes. This method is effective only for slowly varying environments.

(b) The code FEPLS solves broad band pulse problems. It uses a one-way in time approximation of the wave equation. This approach has been used previously in other settings, including Claerbout,[9] and McDonald and Kuperman.[10]

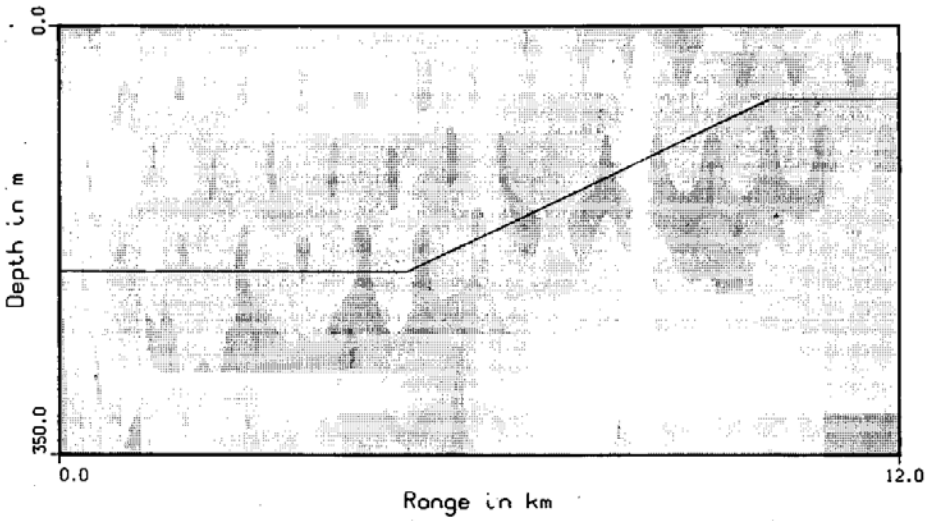

Fig. 5. Contour plot of the propagation loss for Case 3, obtained from a PE code calculation.

Figure 5 shows the results of the FEPE code calculation for our Case 3, the depth outlines of the continental shelf being indicated in the figure. Similar to Fig. 4, the contour lines of Fig. 5 show clearly that bottom-refracted energy does not get lost in the depths, but remains channeled in the sediment, propagating up the continental shelf beneath the ocean floor.

In order to further clarify the mechanism of bottom penetration in the presence of an upward-refracting sound speed gradient in the sediment, we used FEPLS to obtain some results for Case 3 when the source (located at a depth of 112m, at 5 km before the start of the upslope) emitted a Gaussian pulse of the form

$$\frac{A}{r}\exp\left[-\left(\frac{r-ct}{10m}\right)^2\right],$$

c = 1500 m/sec. In our subsequent plots, this pulse is followed along and displayed within a cell 300 m wide by 400m deep that moves with the pulse, containing it in its upper left portion. Figure 6 shows the contour lines of the field, with 0 dB contours marked and with dashed contours indicating negative values of the amplitude. It corresponds to a location of 5000m from the source, at the beginning of the upslope (cf. Fig. 1). The horizontal line in the figure represents the water-sediment interface within the display cell.

The dense contours in the upper left of Fig. 6 represent the primary water-borne pulse; the contours in the lower portion the bottom-penetrating field (note that due to the higher sound speed in the sediment, it has run much ahead of the primary pulse over its 5000m course from the source); and the contours in the upper right the field that has been returned into the water from the preceding sediment-borne field (and multiply reflected there), due to the upward-refraction in the sediment. The right half of Fig. 6 is shown in Fig. 7 on a larger scale and with more finely differentiated contours. It shows the following interesting features. In the center of the water region, one notices a (pulsed) wavefront extending diagonally up to the right (i.e., the pulse propagating towards the lower right). This corresponds to an earlier bottom-penetrating pulse that had been refracted back up into the water, and then reflected downward by the sea surface. One further discerns a directly upward-refracted pulse whose front

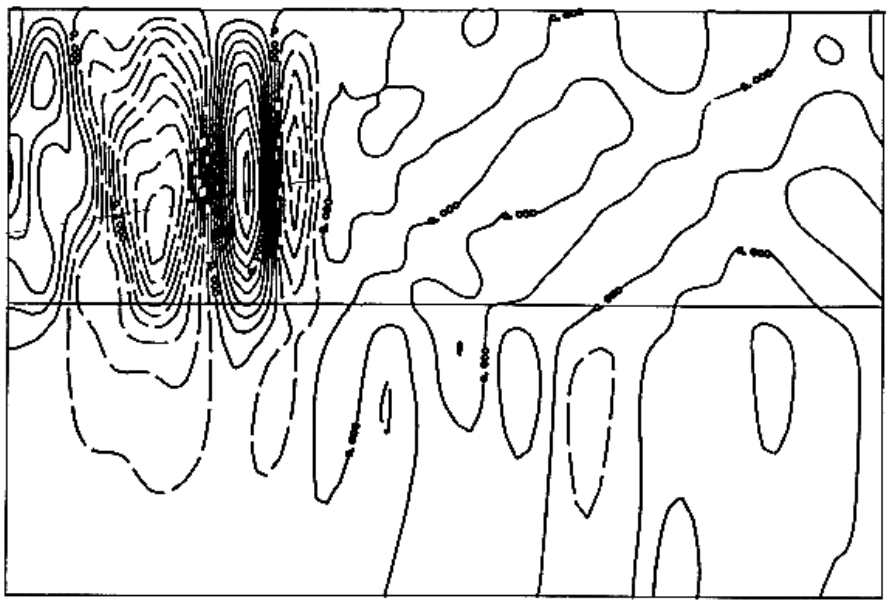

Fig. 6. 300-m wide display cell for a water-borne Gaussian pulse (upper left), bottom-penetrating pulses and multiply-reflected pulses refracted back into the water, located 5 km from the source and at the beginning of the upslope.

starts at the right edge of the figure at the interface, and stretches diagonally up to the left. At the lower right, this front continues into the sediment at a steeper angle given by Snell's law, so that we here see a pulse front in the act of being refracted back up into the water. As mentioned, the in-sediment portion of this front propagates at a speed faster than water-borne sound, so that the water-borne portion of the same front represents a kind of head wave[11] which strails into the water behind the bottom-borne portion of the front.

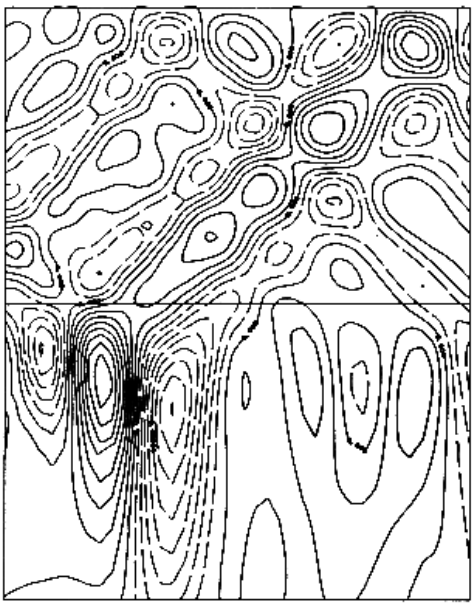

Fig. 7. Right-hand portion of Fig. 6 with more finely differentiated contours.

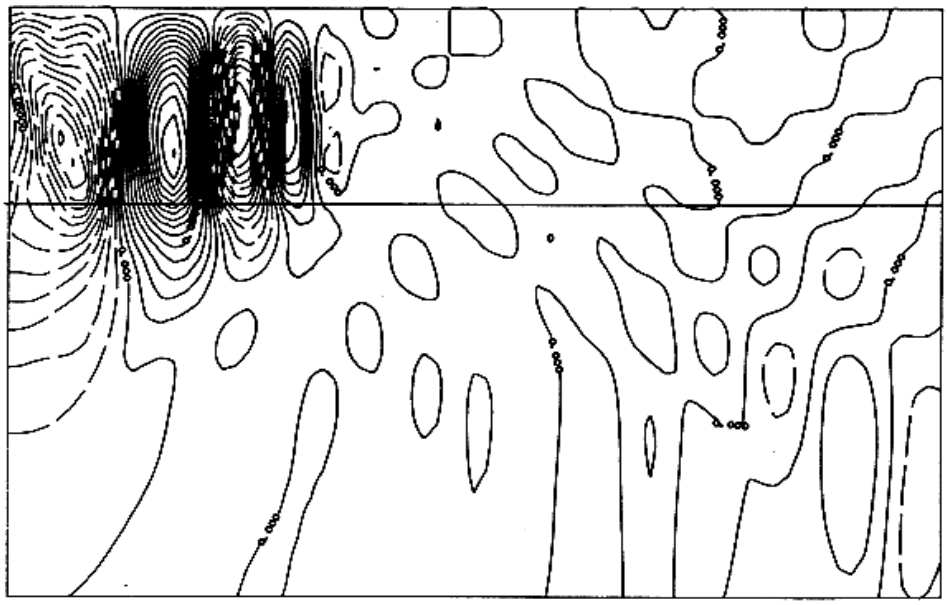

Fig. 8. Similar to Fig. 6, at a location 2500 m into the upslope.

In Fig. 8, we present similar results for the water- and sediment-borne fields in a range cell at a distance of 7.5 km from the source, where the water depth has decreased from 200m to now 132 m. As a consequence, the primary pulse has become squeezed, and the bottom-borne field (not shown separately) is now denser too; i.e., there is still a large amount of bottom-penetrating energy present immediately below the sediment interface.

As noted, due to the large distance (5 km) of the source from the upward-sloping portion to which Figs. 6-8 refer, the fast bottom-penetrating fields have had time to proceed far ahead of the primary pulse, thus filling all the sediment portion of the display cells as well as, by upward refraction, their upper-right portions. In order to catch both the water-borne and the bottom-penetrating primary pulses in one cell, we made a calculation (shown in Fig. 9) for a distance of 500m to the right of the start of the upslope, where the source was now placed at 500m to the left of the start of the upslope. One sees here the leading front in the water (186.5 m deep), the leading front of the sediment-borne pulse (ahead of the water-borne pulse), and trailing behind it a head wave refracted back up into the water at Snell's angle.

In summary, for the isovelocity-bottom case, the water-borne acoustic energy when converted into bottom-penetrating sound upon cutoff, only travels downwards rather than towards the shore. Contradistinctively, we have shown that a positive (realistic) sediment gradient causes the bottom-penetrating sound to travel along the ocean floor, rather than downwards into the basement. Bottom-mounted receivers can thus be expected to register signals originating in the ocean, after traveling up the continental shelf beyond final cutoff, at locations closer to shore than can receivers in the water.

Acknowledgements

Various stages of this work have been supported by the Office of Naval Research, and by the Singer Company, Link Simulation Systems Division.

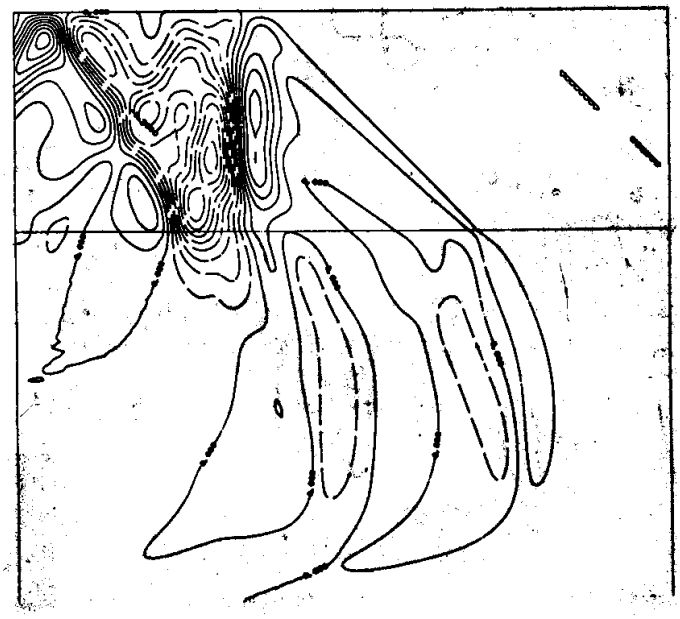

Fig. 9. Similar to Fig. 6, 500m into the upslope and with the source 500 m to the left of the beginning of the upslope.

References

1. J. F. Miller, PhD thesis, Department of Physics, Catholic University of America, Washington, DC 20064, 1985.
2. J. F. Miller, A. Nagl, and H. Überall, Upslope sound propagation through the bottom of a wedge-shaped ocean beyond cutoff, J. Acoust. Soc. Am. 79:562 (1986).
3. F. B. Jensen and W. A. Kuperman, Sound propagation in a wedge-shaped ocean with a penetrable bottom, J. Acoust. Soc. Am. 67:1564 (1980).
4. R. B. Evans, A coupled mode solution for acoustic propagation in a waveguide with stepwise depth variations of a penetrable bottom, J. Acoust. Soc. Am. 74:188 (1983).
5. A. D. Pierce, Guided mode disappearance during upslope propagation in variable depth shallow water overlying a fluid bottom, J. Acoust. Soc. Am. 72:523 (1982).
6. A. D. Pierce, Augmented adiabatic mode theory for upslope propagation from a point source in variable-depth shallow water overlying a fluid bottom, J. Acoust. Soc. Am. 74:1837 (1983).
7. A. Nagl, H. Überall, A. J. Haug, and G. L. Zarur, Adiabatic mode theory of underwater sound propagation in a range-dependent environment, J. Acoust. Soc. Am. 63:739 (1978).
8. Michael D. Collins, Finite-element propagation codes at NORDA (1986), unpublished.
9. J. F. Claerbout, "Fundamentals of geophysical data processing," McGraw Hill, New York (1976).
10. B. E. McDonald and W. A. Kuperman, Time domain solution of the parabolic equation including nonlinearity, Comp. & Math. w. Appl. 11:843 (1985).
11. H. Überall, Surface waves in acoustic, in: "Physical Acoustics" vol. X, W. P. Mason and R. N. Thurston, eds., Academic Press, New York (1973).